

Analysis of Track Support and Determination of Track Modulus

GERALD P. RAYMOND

ABSTRACT

A design methodology that uses an approach similar to that outlined in the American Railway Engineering Association Manual for Railway Engineering for calculating the stresses below crossties of conventional railway tracks is presented. There is discussion of the practical effects of track modulus variability and its possible optimization from the point of view of both static and dynamic loading with particular reference to ballast and subgrade stress levels. These stresses are then used to estimate track deformation. Track deformation may then be used to calculate a conventional track modulus. With such a technique it is possible to calculate the effects of ballast depth variability and compressibility of crossties on track response.

The two main requirements of a stable subgrade are the provision of sufficient granular or soil-modified cover to ensure that overstressing does not occur and the provision of a granular filter blanket to prevent the piping and thus loss of subgrade fines from below the track bearing area. To ensure that overstressing does not occur, the track stresses need to be calculated. A means of calculating these stresses that follows an approach similar to that of the American Railway Engineering Association's Manual for Railway Engineering is outlined herein. Presentation of subgrade stability techniques is beyond the main scope of this work.

STATIC DESIGN OF CONTINUOUS WELDED RAIL

Talbot (1) has demonstrated that the theory of a continuous beam on an elastic support, or, more correctly, a linear spring (Winkler) foundation gives calculated bending moments for the rails close to those measured in freshly tamped track. Many investigations, including extensive ones performed by the Association of American Railways, have confirmed the validity of this theory. The American Railway Engineering Association (AREA) in its Manual for Railway Engineering (2) also endorses this method of analysis (chapter 22, article 3.2, paragraph 3.2.1, section a):

Because of the many variables involved in tie and ballast track, the calculation of track stress and strain cannot be regarded as an exact science. However, in-service tests have shown that the track structure can be analyzed within acceptable limits of accuracy by considering the rail as equivalent to a continuous beam resting upon uniform elastic supports.

This design method results in the representative differential equation for the elastic beam (rail) subject to a vertical (wheel) load (P) of

$$EI(d^4z/dx^4) + Uz = 0 \quad (1)$$

where

- E = elastic modulus of the beam,
- I = second moment of area of the beam,
- z = deflection at a point x from the applied load,
- x = distance along the beam from the point of application of the load, and
- U = modulus of the elastic support commonly known as the track modulus (note that the track modulus as used in common practice and in the AREA manual relates to a single rail).

For a single wheel load (P) on an infinitely long beam the solutions to this equation are well known:

$$z_x = (\lambda P/2U) (\cos \lambda x + \sin \lambda x) \exp(-\lambda x) \quad (2)$$

$$M_x = (P/4\lambda) (\cos \lambda x - \sin \lambda x) \exp(-\lambda x) \quad (3)$$

where

$$\lambda = [U/(4EI)]^{0.25} \quad (4)$$

The maximum values of z and M are directly below the load at x = 0.

$$z_0 = \lambda P/(2U) \quad (5)$$

$$M_0 = P/(4\lambda) \quad (6)$$

These results are normally given in the form of the influence chart shown as Figure 1 in which the distance to zero moment (X_1) is used as a distance base [e.g., exhibit 1 of chapter 22, AREA manual (2)].

$$X_1 = \pi/(4\lambda) \quad (7)$$

Alternatively, but not so commonly, a deformation wavelength of $2\pi/\lambda$ is used. The rail seat loads are commonly calculated as

$$Q_x = z_x U S = (1/2) \lambda S P (\cos \lambda x + \sin \lambda x) \exp(-\lambda x) \quad (8)$$

where S is the spacing of crossties. For a crosstie placed directly below the load (x = 0)

$$Q_0 = P\lambda S/2 \quad (9)$$

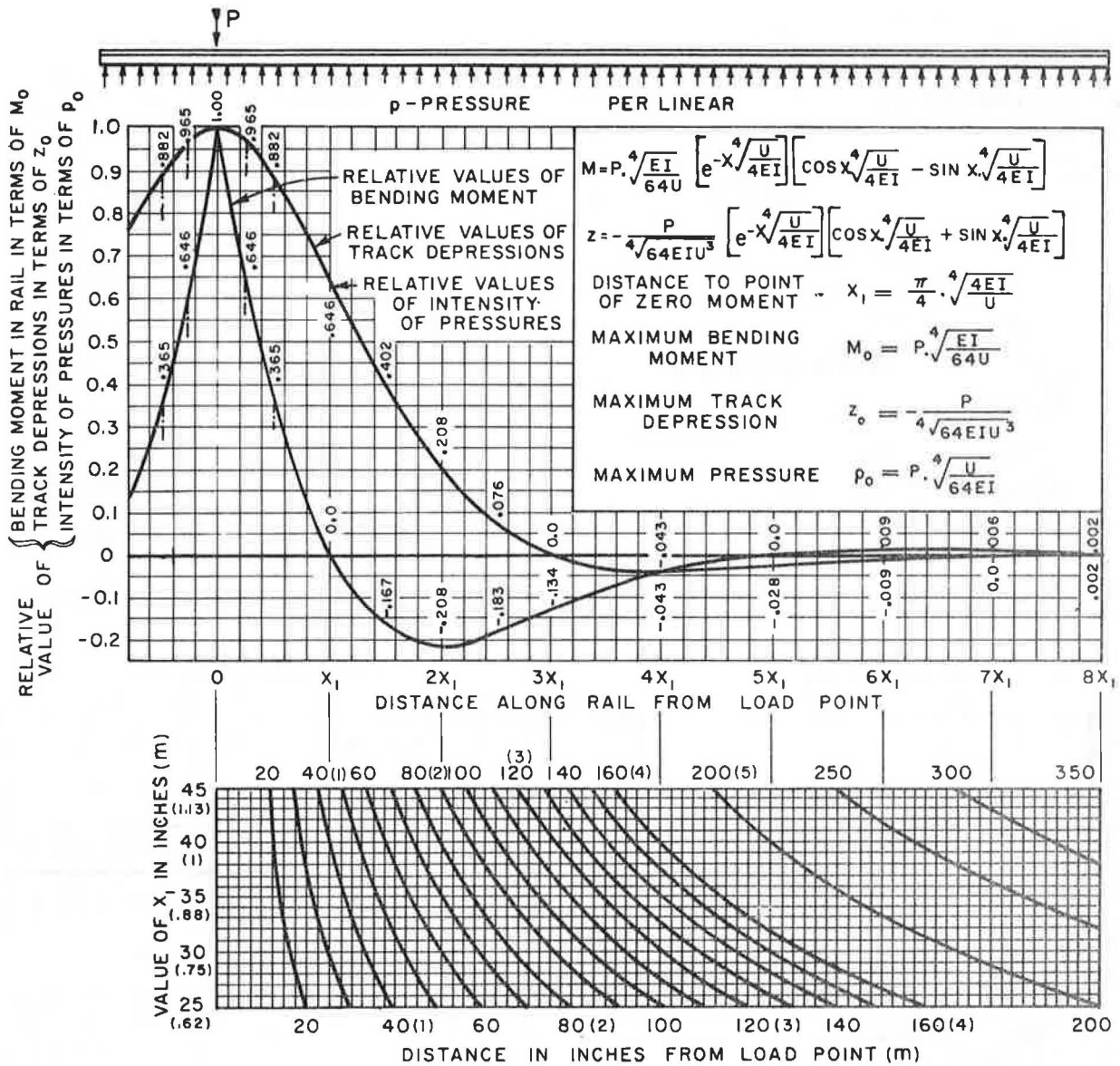


FIGURE 1 Influence chart for track design.

As an example of the effect of track modulus on rail seat loads, Figure 2 shows the variation of the rail seat loads in the vicinity of a single 147-kN (33-kip) wheel load on 68-kg/m (136-lb/yd) rail for two different crosstie spacings in which the central crosstie (crosstie 1) is directly below the load (i.e., the crosstie is positioned to produce a maximum rail seat load). Examination of Figure 2 indicates that, within the limitations of values likely to occur in practice, variation of the track modulus has a much greater influence on the rail seat load than does crosstie spacing.

EFFECT OF MULTIPLE WHEELS OR AXLES

Because the preceding theory is based on elastic response, the theorem of superposition applies and the effect of multiple wheels or axles can be simply calculated as

$$z_j = \sum z_x \tag{10}$$

$$M_j = \sum M_x \tag{11}$$

$$Q_j = \sum Q_x \tag{12}$$

where the different values of x are the distances of each wheel load from the position point j .

Example calculations of the maximum track deflection and maximum rail base bending stress are plotted on Figures 3 and 4 for both a single-axle and two coupled G-75 trucks (wheel spacing 1.78 m, 1.99 m, and 1.78 m or 70 in., 78.5 in., and 70 in.) supported by either 45-kg/m (90-lb/yd) rail or by 68-kg/m (136-lb/yd) rail. Maximum deflection occurs below the interior axles and maximum rail stresses occur below the outer axles. Examination of these curves show that as the track modulus decreases from the region of about 35 to 70 MN/m² (5 to 10 kips/in.²) of rail there is a rapid increase in deflection or rail stress, and if the track modulus increases from this region of values a gradual reduction of deflection or rail stresses occurs. It may be concluded that for statically loaded track 35 to 70 MN/m² (5 to 10 kips/in.²) of rail may be anticipated as an optimized value range of track modulus, at least for initial consideration.

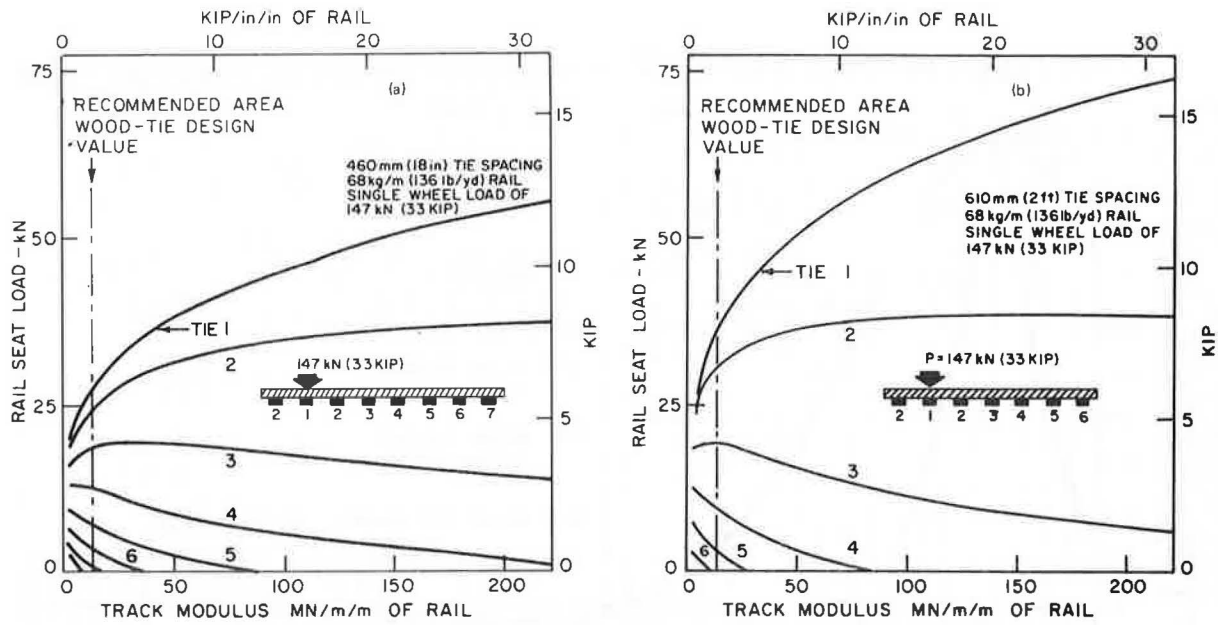


FIGURE 2 Effect of track modulus variation on rail seat loads resulting from a single static wheel or axle load: (a) 460-mm (18-in.) crosstie spacing and (b) 610-mm (24-in.) crosstie spacing.

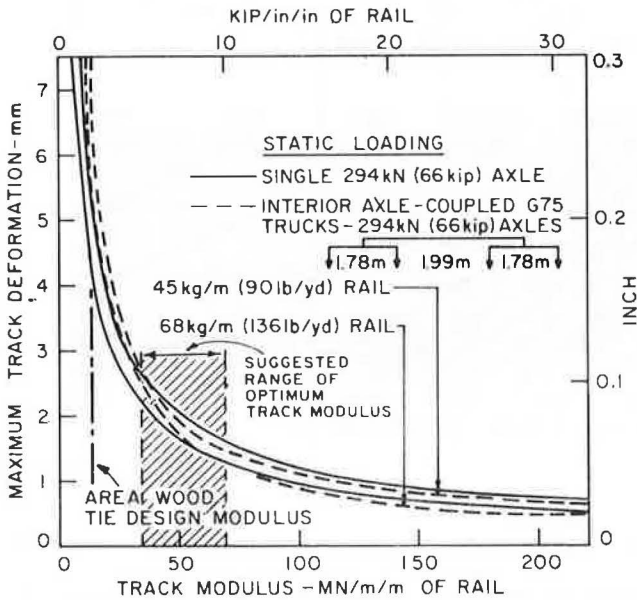


FIGURE 3 Effect of track modulus variation on maximum track deformation.

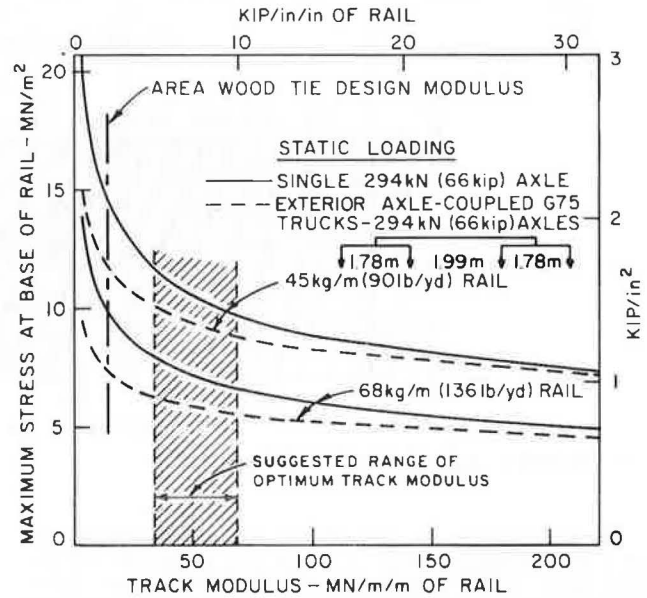


FIGURE 4 Effect of track modulus variation on maximum stress at base of rail.

CALCULATIONS OF STATIC SUBGRADE STRESSES

Similar calculations were made using Equation 12 for the determination of the rail seat loads obtained from multiple axles. The rail seat load may then be used to calculate tie bearing pressures and subgrade stresses. Sufficient evidence is available in the technical literature to show that where soils are unable to resist tensile forces the vertical stress is given by superposition of Boussinesq's solution for stresses within a semi-infinite elastic solid with surface loading. Below each rail seat the crosstie can be assumed to produce a rectangularly loaded area on the ballast. This permits the use of the solutions developed by Love (3) who extended Boussinesq's solution to a rectangularly loaded

area. The area of the crosstie bearing surface per rail seat (A_b) may be calculated according to the AREA manual as

$$A_b \text{ (per rail seat)} = b(\ell - \ell_r) \{1 - [C(\ell - \ell_r)/t^{0.75}]\} \quad (13)$$

where

- b = width of crosstie,
- ℓ = length of crosstie,
- ℓ_r = distance center to center between rails,
- t = thickness of crosstie, and
- C = constant = 0.04 (0.018) if dimensions are in millimeters (inches) (note constant is dependent on units).

Alternatively, the area is assumed equal to some tamper influence distance on either side of the rail. The AREA method results in rail seat bearing areas the width of the crosstie and a length determined by the formula (Equation 13) that results in 879 mm (34.6 in.) for a crosstie 178 mm (7 in.) deep by 2.55 m (8 ft 6 in.) long and 975 mm (38.4 in.) for a crosstie 178 mm (7 in.) deep by 2.70 m (9 ft 0 in.) long. For purposes of illustration two rail seat bearing lengths of 914 mm (36 in.) each below each of two rails spaced 1.50 m (60 in.) centerline to centerline apart have been assumed. This is considered the approximate distance influenced by the tamper tines.

Figure 5 shows the solution obtained using different track moduli of the underlying maximum vertical support stress resulting from a single axle load on 68-kg/m (136-lb/yd) rail and 279-mm (11-in.) crossties spaced at 610-mm (24-in.) centers. The

contact pressure or vertical stress at zero depth for a single axle load may be seen to increase as the fourth root of the track modulus (i.e., an increase of track modulus by a factor of 16 doubles the contact stress). With depth the difference in vertical stress decreases slowly such that, even at 0.8 m (32 in.), the effect of track modulus variation on subgrade stresses from the single axle is considerable.

Figure 6 shows similar calculations, using the same crosstie size and spacing, for two coupled G-75 trucks having 294-kN (33-ton) axle loads. Interaction between axle loads is sufficient under the lower values of track modulus to cause a considerable increase in the contact pressure or vertical stress at zero depth. This reduces the dependence of either maximum contact pressure or maximum subgrade stress on the variation of track modulus. Using the two highest track moduli interaction actually caused

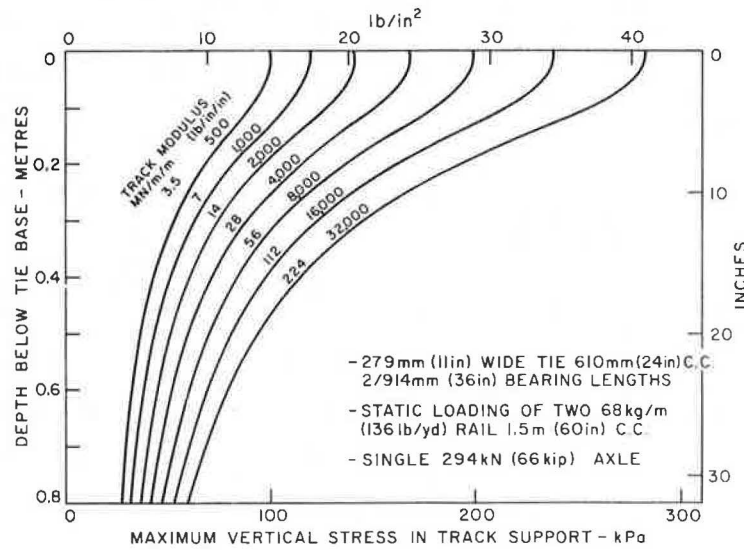


FIGURE 5 Effect of track modulus variation on maximum vertical stress in track support resulting from a single static axle load.

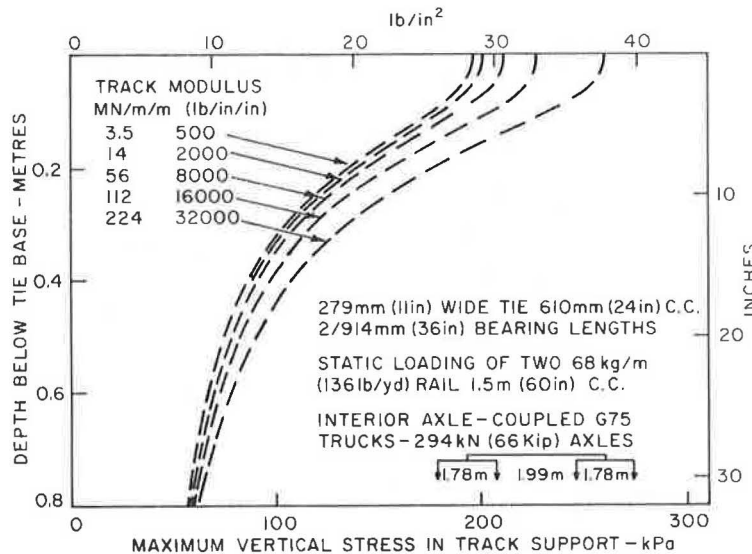


FIGURE 6 Effect of track modulus variation on maximum vertical stress in track support resulting from two coupled G-75 trucks.

a reduction in these maximum values from those calculated for a single axle.

The effect of variation of both track modulus and crosstie spacing is shown in Figure 7. In this figure is plotted the effect of using a 229-mm (9-in.) crosstie at 458-mm (18-in.) centers versus a 279-mm (11-in.) crosstie at 610-mm (24-in.) centers on track having moduli of 14 MN/m² (2,000 lb/in.²) of rail and 224 MN/m² (32,000 lb/in.²) of rail with 68-kg/m (136-lb/yd) rail. If no change is made in track modulus, only about a 10 percent change in contact stress occurs for a change in specified crosstie size and spacing. On the other hand it is clearly evident from Figure 7, and from the maximum rail seat loads shown in Figure 2, that much higher support stresses result from a change in specified track modulus. This effect is more pronounced for a single axle than for coupled G-75 trucks.

In the case of a single axle on 68-kg/m (136-lb/yd) rail changing the modulus from 14 MN/m² (2,000 lb/in.²) of rail to 224 MN/m² (32,000 lb/in.²) of rail causes the crosstie-ballast interface stress, for the same crosstie spacing, to approximately double (i.e., 100 percent increase). Interaction of axles is more pronounced on softer track because the rail is more effective in spreading the load thus reducing the effect of track modulus change on support stresses for the coupled G-75 trucks. Changing the track modulus but retaining the same rail and crosstie size and spacing reduces the increase interface stresses to an increase of approximately 30 percent for the 229-mm (9-in.) crossties and approximately 25 percent for the 279-mm (11-in.) crossties.

In the event of changing from crossties 229 mm (9 in.) wide at 458-mm (18-in.) spacing to crossties 279 mm (11 in.) wide at 610-mm (24-in.) spacing, the effect of modulus change from 14 MN/m² (2,000 lb/in.²) of rail to 224 MN/m² (32,000 lb/in.²) of rail on the interface stress for a single static axle would be an increase of approximately 120 percent. Axle interaction for the two coupled G-75 trucks would reduce this increase to approximately 35 percent.

A point worth noting from Figure 7 is that as the depth increases the support vertical stresses resulting from similar wheel loadings and the same track modulus tend toward similarity. This, of course, is to be expected from "Saint Venant's prin-

ciple," which says that two different distributions of force, having the same resultant acting on a small part of an elastic body, will produce the same stress except in the immediate neighborhood of the loaded part. Thus, provided the ballast is clean and of full section so it can function effectively, changes in crosstie spacing or the size of the bearing area are unlikely to affect the magnitude of the subgrade stresses but would affect the stresses in the ballast. These conclusions are verified in Figures 8 and 9 that show the distribution of support stresses for a single axle using different crosstie spacings and crosstie sizes, respectively. As previously shown, multiple axles decrease the differences shown by single axles and have been omitted from these figures.

At much greater depths than shown on Figure 5 (such greater depths are of little practical significance) the effect of modulus change would also be negligible. As far as normally anticipated ballast depths are concerned, track modulus variation is much more significant in affecting the magnitude of the subgrade stresses than variation in crosstie spacing or bearing area within the normally used limits of these variables. This is not to suggest that changes in crosstie spacing and bearing area do not affect the track modulus but rather that their effect on any change in track modulus (which is not given by the theory) has a greater influence on support stresses than their direct effect from theoretical stress distribution theory assuming no change in track modulus.

Similar calculations, done to show the effect of changing rail mass, are shown on Figure 10. Although there is some effect on the subgrade and ballast stresses for a single axle on the softer track, interaction of wheel loads for the coupled G-75 trucks reduces this difference to a negligible amount. The effect of subgrade stress reduction is much more apparent from a rail mass increase when the track is extremely stiff. This reduction occurs both for the single and the multiple axle case with maximum stresses being less for multiple axles than for single axles on extremely stiff track.

ESTIMATE OF TRACK MODULUS

The solutions developed by Love (3) for a rectangular loaded area allow for the calculation of not

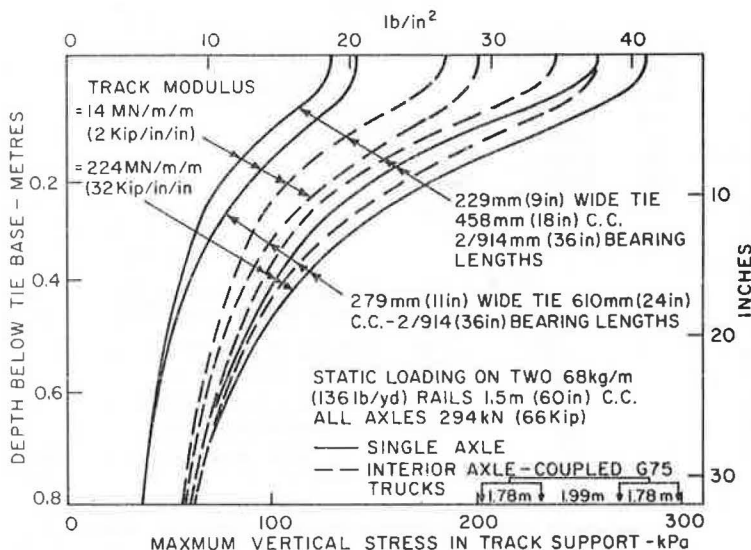


FIGURE 7 Example of effect of major increase in track modulus on maximum vertical stress in track support.

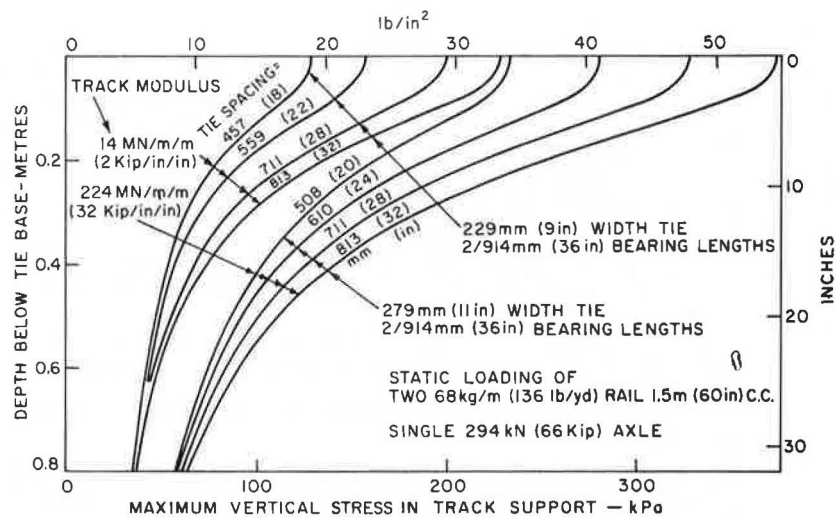


FIGURE 8 Example of effect of cross-tie spacing on maximum vertical stress in track support.

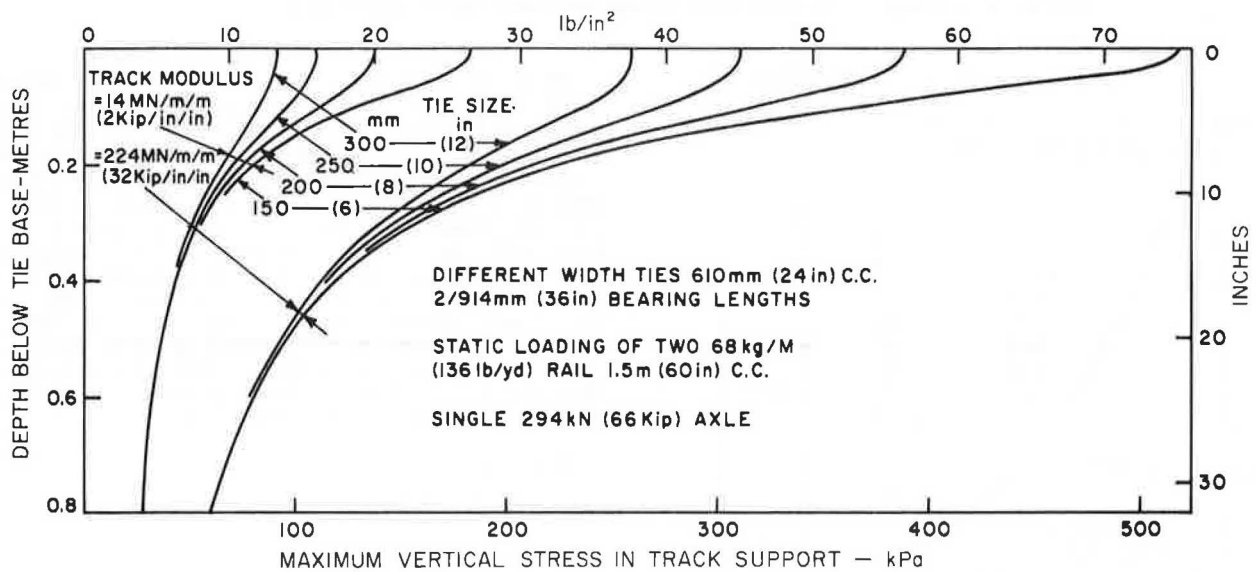


FIGURE 9 Example of effect of cross-tie size on maximum vertical stress in track support.

only the vertical stress but also the six stresses (three normal and three shear) that define the state of stress at any point. Knowing the pseudoelastic parameters of the support soil allows the calculation of the strain at that point, which, by numerical integration, allows the calculation of support deformation. Addition of such deformations to those produced by the rail seat load on the cross-ties via the tie plates allows the total deformation to be estimated for a given set of conditions. Because different track moduli produce different calculated support stresses and rail seat loads, a series of calculations of total deformations using different track moduli is required. These results should then be compared with the deformations predicted by the "beam on elastic support" theory to determine the track modulus that defines identical deformations. It should be clearly understood that the deformation experienced by the rail at the rail seat includes not only the deformation of the track support but also that of the cross-tie and its accessories. An example of the results of such a series of calculations is shown in Figure 11. These results are for a

single axle loading because many field measurements of track modulus are obtained using a long loaded flatcar with two central loading jacks one above each rail. The jacks are used to apply, in increments, the equivalent of a single axle load of different magnitudes. Because of voiding below the cross-tie, the modulus is calculated from the deformation recorded between about 36 kN (8 kips), the weight on an unloaded truck wheel, and 147 kN (33 kips) on each jack.

The results shown in Figure 11 were obtained using 305 mm (12 in.) of clean ballast overlying 610 mm (24 in.) of clean subballast overlying a heavily compacted silt or clay subgrade. The exact compressibility of the subgrade can be expected to vary throughout the year from negligible in extremely dry hot weather to a maximum during extremely wet or thaw conditions if subjected to freezing. Figure 11 represents calculations for extremely dry subgrade conditions. It may be seen that track on such a support constructed with concrete cross-ties and stiff pads would have a track modulus of about 140 MN/m² (20,000 lb/in.²) of rail. Use of the softer

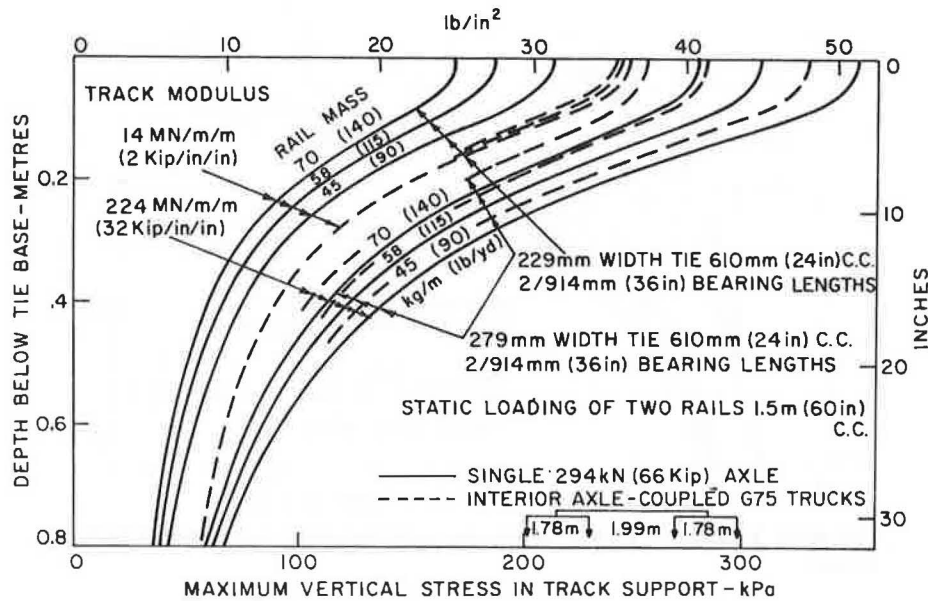


FIGURE 10 Example of effect of rail mass on maximum vertical stress in track support.

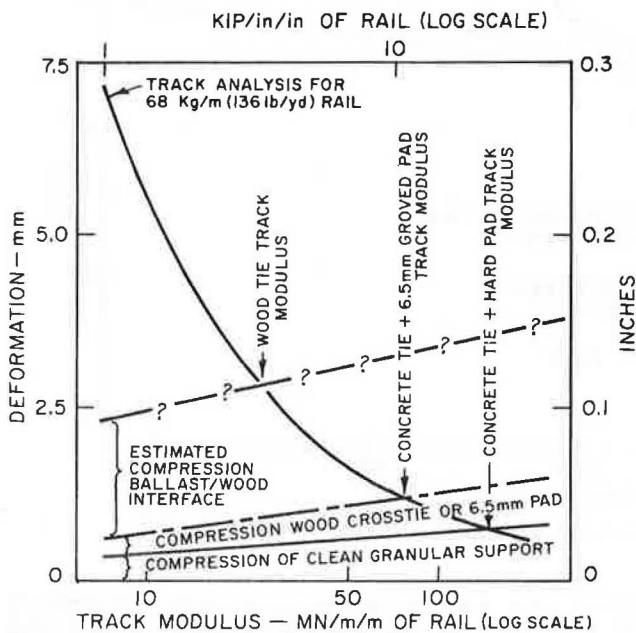


FIGURE 11 Example of estimating track modulus on the basis of pseudoelastic properties of track and support components.

grooved pads recently installed on the U.S. Northeast Corridor reduces the track modulus to about 69 MN/m² (10,000 lb/in.²) of rail. The compressibility of hardwood crossties is similar to that of the softer Northeast Corridor pads; however, the major compression observed in tests on wood crosstie track has been the elastic compression and rebound of the ballast penetration of wood or ballast-crosstie interface. The magnitude of this interface compression is shown on Figure 11 from which it is seen that wood crosstie track has a considerably lower track modulus than does concrete crosstie track. The curves plotted on Figure 11 suggest a track modulus of 24 MN/m² (3,500 lb/in.²) of rail; however, the variability of the interface compression means considerable variation from this value would not be unrealistic.

An alternative method of calculating the deformations from the support alone is to use Steinbrenner's solutions for the settlement of the corner of a rectangular loaded area extended to deal with a layered foundation. Steinbrenner's original solution assumes a homogeneous isotropic elastic layer of constant elastic parameters; thus an extension to deal with layers of different elastic parameters must be used to obtain the same results as are obtained by the use of Love's solution. Both these techniques assume that the stresses, but not the strains, are given by homogeneous elastic theory irrespective of any variations in the soil properties. When the stress distribution has been obtained, the deformations may be calculated from

$$\delta_z = \int \{ [\sigma_z - \nu_i (\sigma_x + \sigma_y)] / E_i \} dz \quad (14)$$

where

- σ = normal stress,
- ν_i = pseudo Poisson's ratio of the soil layer, and
- E_i = pseudoelastic modulus of the soil layer.

The integration is usually done numerically by dividing the foundation into a relatively large number of soil layers and then summing the resulting layer deformations. Note that the pseudoelastic properties of granular soils vary with degree of compaction and the properties of cohesive soils with moisture content or, more correctly, soil suction. In addition, an underlying soft cohesive soil tends to prevent compaction of an overlying granular soil; thus the selection of appropriate pseudoelastic parameters requires considerable judgment. The main point, however, is that once the selection has been made the calculations are relatively simple. Results from typical calculations showing the deformation between the base of the crosstie and the given depth are shown in Figure 12 for a granular layered deposit in a loosely compacted, and in a densely compacted, state making the somewhat simple assumption that the wheel load is taken 50 percent by a central rail seat and 25 percent by adjoining rail seats. Because the calculations assume elastic response, the support deformations are directly proportional

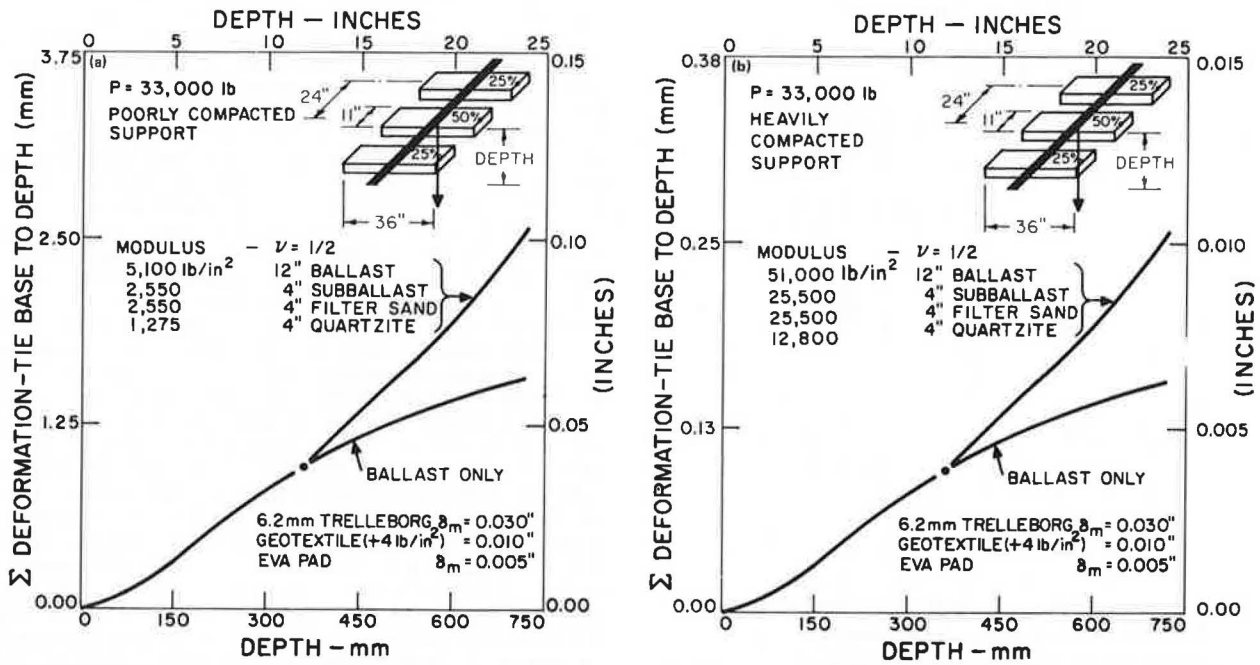


FIGURE 12 Example of simplified estimation of contribution to track deformation of support materials: (a) poorly compacted and (b) heavily compacted.

to any variation in the central rail seat load of 73.5 kN (16,500 lb). The calculations should, of course, be done for the actual distribution of rail seat loads produced by the different track moduli to obtain the best estimate of modulus.

The 50 to 25 percent load distribution does, however, permit a quick rough estimate of track modulus because, from Equation 8,

$$U = Q_0 / (S\delta_0) \tag{15}$$

where Q_0 is the maximum rail seat load for the single wheel load P and δ_0 is the total summation of rail seat deformation at Q_0 . Thus a rough estimate of U can be obtained as

$$U = P / (2S\delta_{50}) \tag{16}$$

where δ_{50} is the total deformation using 50 percent of P as the maximum rail seat load (note Figure 12 shows only the contribution to the total deformation due to the soil support of the shown 610 mm or 24 in. directly below the tie base).

CALCULATION OF DYNAMIC INCREMENT FOR CONTINUOUS WELDED RAIL

Kenney (4) has shown that on perfect track transversed by perfect wheels track forces rise extremely slowly with speed requiring a speed of about 1600 km/hr (1,000 MPH) to reach track resonance. Track irregularities or wheel irregularities are therefore the principal cause of major dynamic track forces given current (1985) speeds. Any complete theory dealing with track and wheel irregularities is clearly complex but because the track mass is much less than the unsprung mass of a wheel set it appears reasonable to neglect the track mass as a first approximation and to take the effect of the suspension spring as a steady force. The equation of motion then reduces to

$$M(dw^2/dt^2) + K(w + s) = 0 \tag{17}$$

where

- w = displacement of the unsprung mass from the static equilibrium position,
- s = amplitude of the irregularity,
- M = unsprung mass, and
- K = track stiffness.

Track stiffness is related to the track modulus by

$$K = (64 E I \bar{v}^3)0.25 \tag{18}$$

The solution to Equation 17 leads to a relationship for dynamic increment of load of the form

$$P_d - P_0 = C s (M K)^{0.5} f(V) \tag{19}$$

where

- P_d = dynamic wheel load,
- P_0 = static wheel load,
- C = a proportionality parameter, and
- $f(V)$ = a function of speed.

For a well-maintained track made of continuous welded rail that is not corrugated the major track or wheel irregularity is believed to be due to wheel flats. Data on wheel flat impact obtained by the Association of American Railroads (5) on wheel flat impacts along with a first trial solution of Equation 19 are shown in Figure 13. According to Equation 19, for any given speed and weight of rail the dynamic increment should increase linearly with the irregularity depth. Because the wheel flats were carefully made as square flats, the irregularity increases with flat length as shown. This is seen as in reasonable agreement with the data considering the scatter in the results. Also from Equation 19, for any given speed the axle load should make no difference to the dynamic increment obtained from a given wheel flat and this is reflected in the theo-

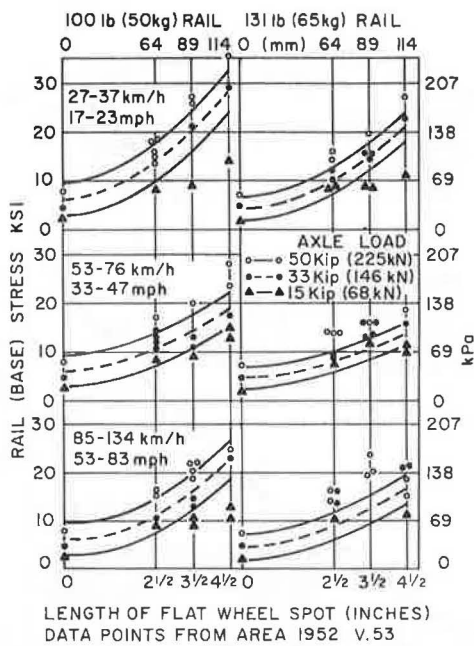


FIGURE 13 Comparison of simplified theory for flat wheel spot with experimental field data obtained by Association of American Railways.

retical curves shown. Thus, from the test data obtained, the dynamic increment for wheel flats from other vehicles and other track constructions may be obtained as

$$P_d - P_o \text{ is proportional to } M^{0.5} U^{0.375} \quad (20)$$

The data of Figure 13 were obtained using a 70-ton (net) freight car with an unsprung axle mass of 1705 kg (3,750 lb) on wood crosstie track. One hundred ton (net) cars with 20 percent heavier axle loads are in more common use today (1985). These cars have an unsprung axle mass of about 1977 kg (4,350 lb)

that suggests an 8 percent increase in impact loading on wood crossties. For concrete crosstie track with stiff pads and stiff subgrades (e.g., dried out clay), the dynamic increment is estimated at an additional 98 percent, whereas soft pads would reduce this increment to 55 percent. For 100-ton cars on concrete crosstie track the increment would be 105 and 59 percent for the stiff and soft pad, respectively. However, due to the nonlinear compression of the components of the track structure, the difference in track moduli for wood and concrete crossties to be applied to the dynamic increment is probably not as numerically diverse as shown in Figure 11 because the track has been compressed by the dead load when the impact of the wheel flat occurs.

Field data in support of differences of dynamic wheel increment associated with different track stiffness, assembled from published data for passenger train wheel loading on the U.S. Northeast Corridor (NEC), are shown in Figure 14 (6,7). It may be seen that more than 90 percent of all wheels give similar loadings consistent with near-perfect wheels on track of similar roughness. The few percent of wheels having major imperfections are those, according to theory, that would show major differences in dynamic increment and this difference is seen (Figure 14) to be largest between wood crosstie track and concrete crosstie track. Although the differences in measured wheel load on concrete crosstie track are small but nevertheless measurable, the effect of a softer track on the rail seat bending moments of the differently padded concrete crossties is clearly evident. Because of the better load-spreading capability of the same rail section on softer track, the bending moments associated with softer pads are considerably less than those associated with the stiffer pads when the dynamic increment becomes large (i.e., at small occurrence levels). It is understood that the experimental results have (rightly according to theory) led to the adoption of softer pads for all further concrete crosstie installations on the NEC and the use of flat wheel detectors as an addition to the normal visual inspection that forms part of normal railroad practice for restricting the access of wheels with flats to track. It is clear

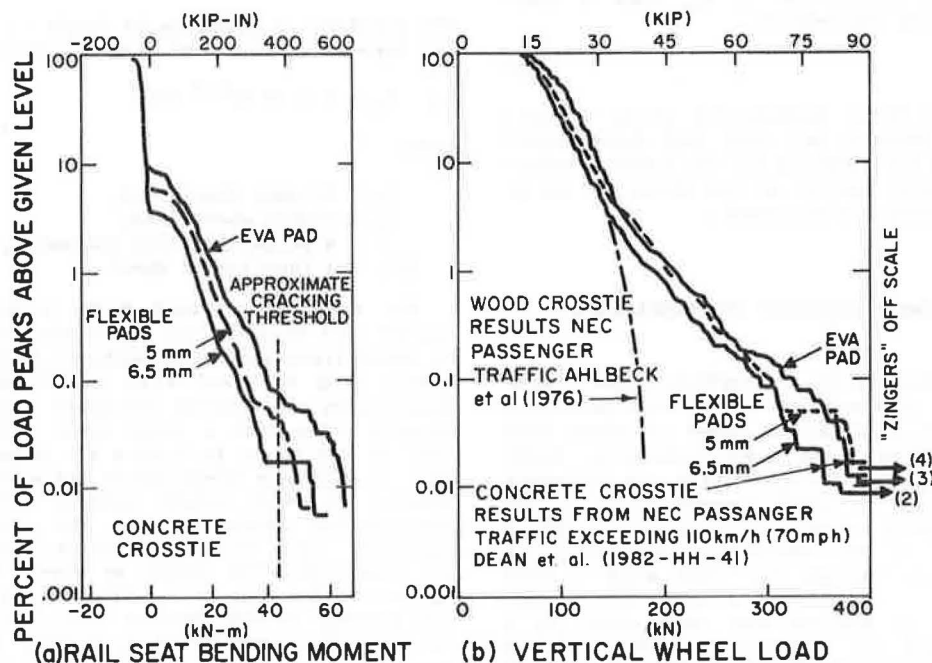


FIGURE 14 Measured dynamic wheel loads for Northeast Corridor passenger traffic (6,7).

that, although no optimization of track modulus has been established or is evident for dynamically loaded track, there is a penalty to be paid by over-stiffening track that is subject to wheel and rail irregularities, which presently (1985) is occurring on North American track. Optimum track stiffness for dynamic loading is probably less than that for static loading.

have been measured and thus the calculation illustrates the negative effect of having extremely stiff track associated with the high unsprung mass of freight vehicles.

TYPICAL STATIC PLUS DYNAMIC SOLUTION

Figure 15 shows results from a typical calculation based on a 51-mm (2-in.) square flat on both wheels of one inside axle of two fully loaded coupled G-75 trucks (i.e., 30-tonne or 66-kip axle load) for three track conditions. The 51-mm (2-in.) flat is the maximum permitted by Association of American Railroad (8) recommendations. The track conditions were track made from wood crossties 229 mm (9 in.) wide with 458-mm (18-in.) spacing giving an assumed track modulus of 14 MN/m² (2 kip/in.²) of rail; track made from concrete crossties with soft pads 279 mm (11 in.) wide with 610-mm (24-in.) spacing giving an assumed track modulus of 84 MN/m² (12 kip/in.²) of rail; and track made from similar crossties with stiff pads giving an assumed track modulus of 224 MN/m² (32 kip/in.²) of rail.

BALLAST DEPTH DESIGN

Clearly evident from Figure 15 is the dramatic effect that a higher track modulus has on the dynamic increment. Fortunately concrete crosstie track and its higher track moduli are generally associated with firmer, and thus generally stronger, subgrades. In addition, wheels do not generally have carefully made square flats associated with "worst conditions." Thus stresses as high as the upper limit shown on Figure 15 are the exception not the rule. Typical foundation design is often based on dead load plus some percentage (often 50 percent) of the live load; the reasoning is that safe bearing stresses include some measure of safety factor and may thus be exceeded on a limited basis. As an example, the Manual for Railway Engineering of the American Railway Engineering Association (2) suggests a dynamic increment of approximately 1 percent of static loading for each 1.6 km/hr (1.0 MPH) of the maximum track speed although the writer would question the sufficiency of the recommendation for the more recently introduced stiffer concrete crosstie track. On the basis of percentage live load chosen, the limits, after proportioning, may be related to the safe bearing stress established for the subgrade soil in question to obtain the required granular (subballast plus ballast) design depth. Figure 16 shows the typical safe bearing stress values or related empirical test values developed for use in highway and airport design (9), both of which require much smaller surface deflection than do railways for good performance. Because railroads are more flexible than major highways it is this writer's opinion that the limits shown in Figure 16

Figure 15 shows the static loading conditions for the maximum vertical support stress along with a combination of both static and dynamic conditions. The total dynamic axle (static + increment) loads for the three assumed moduli were calculated as 294 kN (66 kips), 447 kN (100 kips), and 926 kN (208 kips), respectively. These values are likely to be higher than generally measured in track because wheel flats are never square in practice and are normally taken out of service before becoming the maximum allowable. The concrete crosstie moduli are also somewhat higher than estimated in Figure 11. These higher values were used because such values

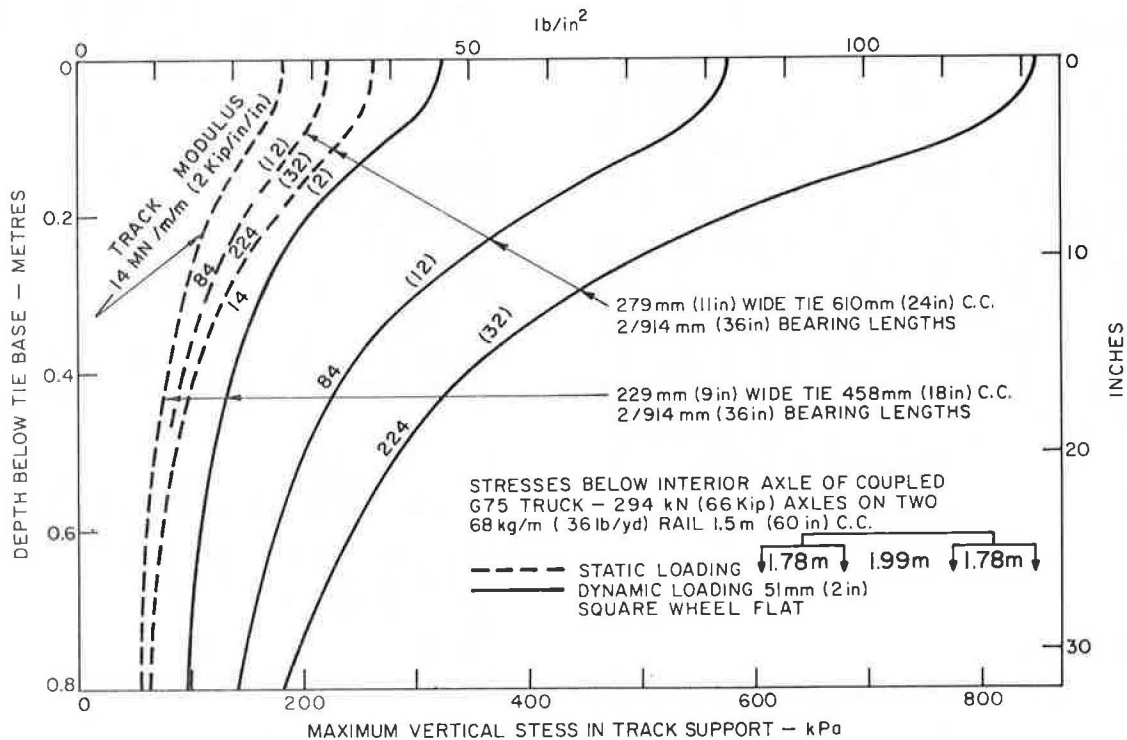
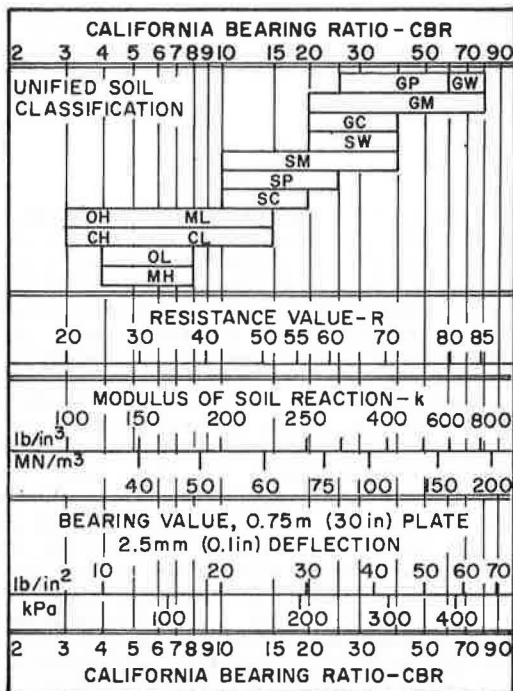


FIGURE 15 Static and dynamic loading from 51-mm (2-in.) square wheel flat effect on calculated vertical track support stresses.



APPROXIMATE INTERRELATIONSHIPS
AT MODIFIED MAXIMUM DENSITY

FIGURE 16 Safe bearing stresses developed for
highway and airport design (9).

are conservative limits for use in track support subgrade design and could probably be increased 50 percent. In addition, where climatic conditions result in freezing temperatures, minimum granular cover equal to at least half the depth of frost penetration is generally specified.

BALLAST STRESSES

It is quite obvious from the data presented that as the track modulus increases, so do the stresses in the ballast, particularly those close to the cross-tie bearing area. Because a higher modulus is associated with concrete crossties than with wood crossties, it is not surprising that higher quality ballast is generally specified when concrete crossties are used. In addition, most concrete crossties are made with silica sands composed of minerals having a Mohs hardness greater than 6. To prevent mineral-to-mineral abrasion, or ballast powdering at the crosstie surface, the ballast must be composed of minerals of similar hardness. Thus ballast for concrete crossties must be obtained from hard mineral tough aggregate. This is best assured by conducting "thin section analysis" on proposed aggregate sources. Thin section analysis also enables the rejection of aggregates that have extensive micro-fractures and former fractures bonded with weak secondary minerals that weather quickly.

SUMMARY AND CONCLUSIONS

A design methodology for calculating stresses below conventional railway crosstie tracks has been presented. Rail seat loads were calculated from the beam on elastic support. The rail seat loads were assumed to cause a rectangular pressure distribution on the ballast from which stresses were calculated using isotropic elastic theory for the distribution

of stresses. These stresses were used to calculate strains on the basis of pseudoelastic properties for the different soil layers. The resulting deformations that were calculated to increase with an increase in track modulus were compared with the deformations from beam on elastic support theory whose deformations decrease with an increase in track modulus. It is suggested that the best design track modulus occurs where both solutions result in the same deformations (assuming correctness of estimated component track properties). An optimum track modulus based on static loading is suggested to occur at about 35 to 70 MN/m² (5 to 10 kip/in.²) of rail, and this is regarded as possibly too high on the basis of dynamic loading for present (1985) North American track and vehicle standards.

It is shown theoretically that the variation of track modulus has a major effect on the track component stresses and that limited field data support the theoretical conclusions.

ACKNOWLEDGMENT

The work reported forms part of general studies funded partly by Canadian Pacific Rail, Canadian National Rail, Via Rail, and Transport Canada Research and Development Centre through the Canadian Institute of Guided Ground Transport and partly by the Natural Science and Engineering Research Council of Canada.

REFERENCES

1. Stresses in Railroad Track--The Talbot Reports. American Railway Engineering Association, Washington, D.C., 1980 (reprint of Report of the Special Committee on Stress in Railroad Track, 1918-1940, A.N. Talbot, chairman).
2. Manual for Railway Engineering. American Railway Engineering Association, Washington, D.C., Vols 1 and 2, 1984.
3. A.E.H. Love. The Stress Produced in a Semi-Infinite Body by Pressure on Part of the Boundary. Philosophical Transactions of the Royal Society, Series A, London, England, Vol. 228, 1928, pp. 377-420.
4. L.T. Kenney. Steady State Vibrations of Beam on Elastic Foundation for Moving Load. Journal of Applied Mechanics, Vol. 76, 1954, pp. 359-364.
5. Effect of Flat Wheels on Track and Equipment: Abstract of Report of Mechanical and Engineering Divisions of the Association of American Railroads. Bulletin 53, American Railway Engineering Association, 1952, pp. 423-448.
6. F.E. Dean, D.R. Ahlbeck, H.D. Harrison, and J.M. Tuten. Effect of Tie Pad Stiffness on the Impact Loading on Concrete Ties. Proc., 2nd International Heavy Haul Conference, Pueblo, Colo., 1982.
7. D.R. Ahlbeck, H.D. Harrison, R.H. Prause, and M.R. Johnson. Evaluation of Analytical and Experimental Methodologies for Characterization of Wheel/Rail Loads. Interim Report PB 272 063. U.S. Department of Transportation, 1976.
8. Manual of Standards and Recommended Practice, Section G, Part II, Wheel and Axle Manual. Association of American Railroads, Washington, D.C., 1984.
9. Soil Primer Handbook. Portland Cement Association, Chicago, Ill., 1956.